Title

Multi stage and illumination dependent segregation in MAPb(I,Br)3

Authors

Babbe, Finn
Masquelier, Eloïse
Zheng, Zhi
et al.

Publication Date

2020-08-21

DOI

10.1117/12.2568995

Peer reviewed

Multi stage and illumination dependent segregation in $MAPb(I,Br)_3$

Finn Babbe[a], Eloïse Masquelier[a], Zhi Zheng[a,b] and Carolin M. Sutter-Fella[a]*

[a] Chemical Sciences Division, Joint Center for Artificial Photosynthesis, Lawrence Berkeley National Laboratory, Berkeley, USA; [b] Berkeley Extension, University of California Berkeley, Berkeley, USA; *csutterfella@lbl.gov

ABSTRACT

An unsolved problem of mixed halide perovskites is the light induced compositional instability. Under illumination microscopic clusters with a higher iodide content form which act as efficient recombination centers reducing device performance. In photoluminescence measurements this leads to the development of a secondary low energy peak that increases in intensity and gradually red shifts. Different theories about the origin have been developed but the underlying key mechanisms are still under debate. In the present study the photoluminescence evolution of $MAPb(I_{0.5}Br0_{.5})_3$ perovskites with varying microstructure is investigated under varying excitation densities. We find a multi stage segregation mechanism with an intermediate stage between the commonly reported mixed phase and the appearance of the I-rich clusters (Br content < 50%). In this intermediate stage nearly I-pure domains (Br content < 25%) form. Using low excitation densities, the interplay between these I-rich clusters and nearly I-pure domains leads to a blue shift of the conjunct I-rich luminescence peak. At high excitation densities the nearly I-pure domains and the I-rich clusters are clearly distinguishable, due to a stronger PL response of the nearly I-pure domains. With continuous illumination more I-rich clusters form acting as carrier traps and recombination centers. Due to this, the influence of the nearly I-pure domains on the PL signature decreases resulting in the commonly reported red shift of the I-rich clusters during halide segregation. To explain our observations, we suggest the existence of I-Br clusters with dynamically changing halide ratio and detailed kinetics depend on microstructure as well as illumination density. The formation of the nearly I-pure domains is fully reversible in the dark and occurs at room temperature and elevated temperatures. Measurements on samples with varying grain size further indicate an enhanced formation of the nearly I-pure domains in samples with high grain boundary density possibly related to a faster halide mobility.

Keywords: mixed halide perovskites, halide segregation, photoluminescence, I-rich domains

1. INTRODUCTION

Over the last decade research in mixed halide perovskites surged based of their favorable optoelectronic properties including high absorption coefficients,[1,2] bandgap tunability,[3–5] high carrier diffusion length,[6–8] and large defect tolerance[9,10] making them attractive for photovoltaic technologies[11,12] and other optoelectronic applications such as LED's,[13,14] photocatalytic devices[15] or lasers.[16] In particular, wide bandgap semiconductors are needed for top cells in tandem photovoltaics and as driver of photocatalytic reactions. The bandgap can be tuned over a broad range in the visible spectrum via halide alloying for example as in $MAPb(I_{1-x}Br_x)_3$ (methylammonium lead iodide bromide) matching those requirements.[3] Device performance of mixed halide perovskites is however hampered by compositional instabilities under illumination in which segregated phases of low and high bromide content form.[17,18] Since the first report by Hoke et al.[17] this phenomenon has been widely studied[17,19–25] and recent reviews can be found by Knight et al.[26] and Brennan et al.[27] Several mechanisms driving halide segregation were hypothesized including pathways to mitigate it, but no holistic picture of the process has evolved so far.

A common way of studying the segregation is by photoluminescence measurements, where in general 2 stages are observed. In the first stage the PL spectra consists of one peak corresponding to the well mixed perovskite phase. Shortly after a secondary peak at lower energies appears which increases in intensity and continuously shifts towards lower energies.[17,22,28] The extend and kinetics of this process have been reported to be dependent on the excitation density,[29] excitation energy,[30] laser repetition rate,[31] surrounding atmosphere,[31] temperature,[17,32] grain size,[33–35] and

composition.[26,27] Under sufficiently low excitation densities halide segregation is not observed, indicating a certain threshold needed to trigger the segregation.[20,32,37,38] Moreover, an enhanced segregation is observed with increasing excitation density[29,31] but also stabilization effects showing a higher final Br content have been reported.[36]

Recently a more complicated process proceeding via multiple stages has been reported.[36,39,40] In particular, a short lived intermediate emission at very low energies appears first showing a blueshift followed by the typically observed gradual redshift. This very low energy peak is proposed to originate from I-rich or I-pure domains (Br content < 25%).[36] Although only a few of those domains exist, a large portion of the radiative recombination is channeled through them due to their low bandgap and likely high quantum efficiency.[36] Over time other I-rich clusters with higher Br content (> 25%) form adding radiative recombination channels and outnumbering the nearly I-pure domains. Further it is speculated that the domains grow in size and incorporate more defects resulting in a reduced radiative efficiency.[36] Both effects lead to a decay in the luminescence of the nearly I-pure domains, leaving the I-rich clusters as main contribution to the overall I-rich luminescence signal. The PL of the I-rich clusters corresponds to the classically observed peak during halide segregation ("Hoke effect"). The overlay of both I-rich peaks (nearly I-pure domains + I-rich clusters) in the intermediate stage leads to a blue shift in the conjunct PL peak as recently shown.[39] This blue shift has been correlated to the microstructure, indicating that the formation of domains is more likely in films that exhibit a large grain boundary density.

Notably, light induced halide segregation is a complex phenomenon where proposed mechanisms can be interdependently connected. In this regard, excitation density dependent segregation with illumination density > 1 sun has not been studied widely nor is it critically relevant for photovoltaic applications, however, a fundamental understanding of underlying processes can only be derived from a systematic investigation of halide segregation dynamics with varying power densities. Therefore, we investigate the initial stages of halide segregation under different excitation densities spanning from 0.1 to 5 suns to probe photon-density dependent radiative emission of mixed $MAPb(I_{0.5}Br_{0.5})_3$ perovskites with varying film microstructure.

For excitation densities of 0.5 suns and below we find a complex segregation in 3 stages similar to recent reports.[39] The blue shift in the intermediate stage II is enhanced for samples with high grain boundary density indicating an increased formation of nearly I-pure domains for samples with low average grain size. For excitation densities above 5 suns more convoluted PL signatures are observed. PL contributions from the nearly I-pure domains are more pronounced possibly related to a larger number of domains formed and the bimolecular nature of the radiative recombination taking place at bandgap minima due to charge carrier funneling and carrier trapping. Since the intensity of the nearly I-pure domains is much higher a distinct emission peak at 1.68 eV can be detected corresponding to a Br content of ~20 %.[3,5] Over time the luminescence of this peak gradually reduces likely due to the formation of I-rich clusters (Br ~ 40 %) with local bandgap minima acting as recombination centers reducing the charge carrier density within the domains. Overall, we suggest the existence of I-Br clusters with varying halide ratio. For samples with low average grain size the increase in intensity of the nearly I-pure domains at the beginning of the segregation process is stronger than in sample with larger grain size. This indicates a correlation between formation likelihood of those domains and grain boundary density. It is speculated that this is mediated by a faster halide mobility along the grain boundaries.

Our findings show that independent of illumination density and sample morphology the segregation proceeds in 3 stages instead of 2 as previously reported. In the first stage we find two independent and competing processes. The first one is the continuous formation of I-rich clusters which gradually reduce in Br content. This process is the commonly observed pathway.[17,20,29] In the second process a few small nearly I-pure domains form with a composition close to $MAPbI_3$. This second process is enhanced in samples with high grain boundary densities as well as at high excitation densities. The third stage is the known gradual red shift of PL emission energy.

2. EXPERIEMENTAL SECTION

Perovskite thin films are fabricated by a solvent engineering process in the glovebox. Precursor solutions are prepared by mixing MAI (Greatcell), MABr (Sigma Aldrich), PbI_2 (TCI) and $PbBr_2$ (TCI) in equimolar ratio in dimethylformamide (DMF) to form $MAPb(I_{0.5}Br_{0.5})_3$. All chemicals are used as received. Before spin coating, 50 µL of precursor solution is applied on a 1.2 x1.2 cm^2 glass substrate. This step is followed by spinning at 1000 rpm for 5 s and 5000 rpm for 35 s. After 9 s, 200 µL of the anti-solvent chlorobenzene is dispersed onto the surface. Subsequently, the samples are annealed on a hot plate at 100 °C. To modify the average grain size, the annealing duration is varied between 30 s (~80 nm grain size referred to as 'small grains') and 10 minutes (~150 nm grain size referred to 'larger grains'). To protect the sample

surface a PMMA (poly(methyl methacrylate)) layer is deposited on the films after they were allowed to cool down to room temperature.

Scanning electron microscope (SEM) images are collected using a FEI Quanta FEG 250 with an acceleration voltage of 5 kV to investigate microstructure and grain size. X-ray diffraction patterns are measured using a Rigaku SmartLab X-ray diffractometer to verify phase purity. Photoluminescence measurements are performed in a home built set up using a solid-state laser (532 nm, r = 0.1 mm) for non-confocal excitation. The emitted PL is collected by a 50x objective, focused onto an optical fiber, guided to a monochromator, and detected spectrally resolved by a silicon detector array (QE Pro). Measured spectra are background corrected and transformed into energy space using Jacobian transformation.[41] The excitation density is varied between 3 / 15 / 150 mW/cm^2 corresponding to 0.1 / 0.5 / 5 equivalent suns. The calculation for the equivalent suns takes the number of photons into consideration which would be absorbed by the materials under illumination with an AM1.5 spectrum as well as the number of photons in the monochromatic excitation light. In literature it is common to take 100 mW/cm^2 laser excitation as 1 sun, but this can be misleading especially when comparing different excitation wavelengths. PL spectra are measured continuously over 120 s at ambient conditions. PL spectra are taken every 0.1 s for excitation densities of 0.5 and 5 suns. Spectra are taken every 0.5 s when measuring at 0.1 suns to improve the signal to noise ratio.

3. RESULTS & DISCUSSION

Top view SEM images of MAPb($I_{0.5}Br_{0.5}$)$_3$ films with different grain sizes (~80 and ~150 nm) and corresponding grain size distribution histograms are shown in Figure 1a-d). For convenience reasons we distinguish the samples by labelling them with 'small grains' and 'large grains' although 150 nm average grain size is still comparably small given that grain sizes of up to several micrometers were reported in literature.[12] The goal here was to not use any additive or other grain size enhancing strategy that might additionally influence the trap density and thus the halide segregation process. Analyzing the films with XRD no secondary phases like PbI_2 are detected as shown in Figure 1e). The main peaks of the 'large grain' sample have slightly narrower full width at half maximum (FWHM) and higher intensities, as one would expect for a better crystallinity.

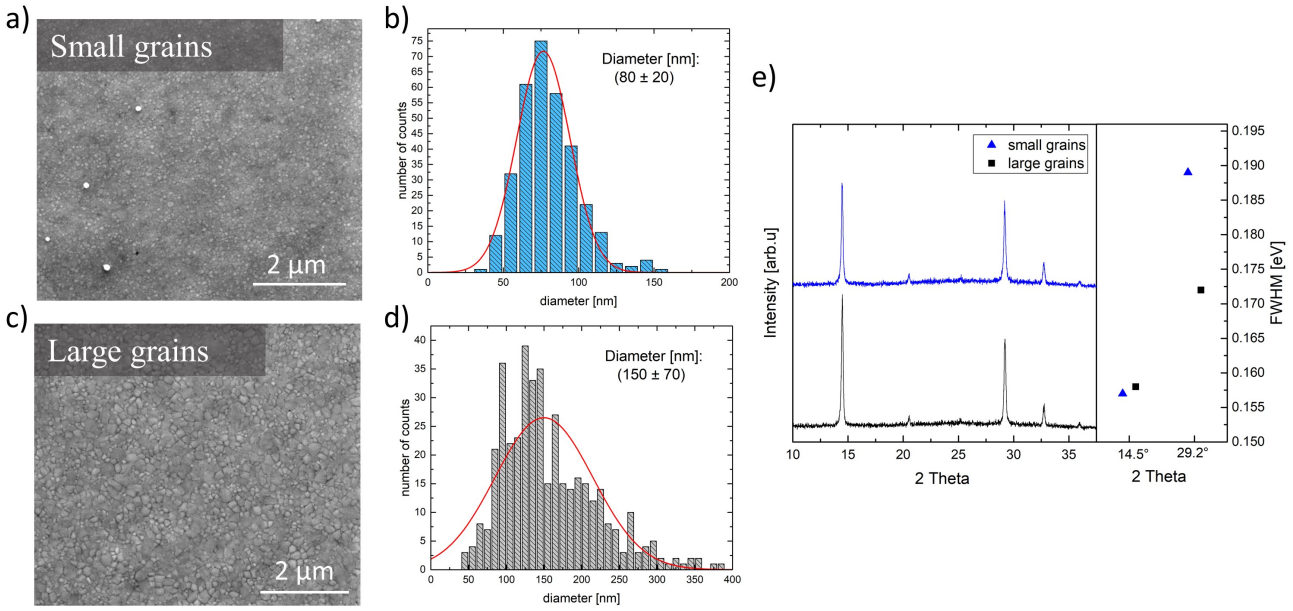

Figure 1. a-d) Exemplary SEM images of a sample with 'small grains' and a sample with 'large grains' as well as their respective grain size distribution. e) X-ray diffraction patterns of the same films as well as the FWHM of the two main peaks.

The evolution of the photoluminescence measured on the sample with 'small grains' under 0.5 sun illumination is shown in a contour plot in Figure 2a) in which each spectrum is normalized to its respective maximum to better visualize peak shifts. In addition, several individual PL spectra are plotted linearly in Figure 2b). For the first few seconds a peak at

1.87 eV is observed corresponding to the photoluminescence of the well mixed perovskite phase with 50% Br.[3] After a couple of seconds a secondary peak at lower energies (~1.7 eV) appears which quickly grows in intensity. This peak is related to luminescence from light induced I-rich clusters.[17] The low energy peak then shifts towards higher energies in stage II (Figure 2a), which differs from the commonly reported gradual red shift of the low energy peak.[17,20] This red shift appears only after ~25 seconds of illumination (here labelled as stage III). We described the multi stage segregation process in 3 instead of 2 stages previously and linked it to the superposition of luminescence from clusters of varying Br content.[39] Initially a flash formation of the nearly I-pure domains takes place as was shown by Suchan et al.[36] Due to the low bandgap of the nearly I-pure domains a majority of the radiative recombination takes place there. There is no measure of the domain density but it was speculated that there are few and they are separated by several micrometers.[36] Over time more and more I-rich clusters with higher Br content form under illumination. Those clusters have a higher bandgap but greatly outnumber the nearly I-pure domains, leading to their appearance in the luminescence spectrum. As another plausible explanation, the density of nearly I-pure domains decreases over time due to a transient change in halide content. The luminescence from the different I-rich clusters greatly overlap and therefore only one joint I-rich luminescence peak (~1.72 eV) is observed. The luminescence of the I-rich clusters with higher Br content strongly increases over time, leading to a peak broadening as well as the blue shift observed in stage II.[39] Then in stage III the commonly observed red shift accompanied by a further increase in intensity is detected.

The magnitude of the blue shift in stage II has been correlated to the average grain size showing an increasing blue shift with decreasing grain size.[39] The blue shift in stage II is much smaller in the 'large grain' sample measured under 0.5 suns (Figure 3e) but is still detectable as indicated by the stars.

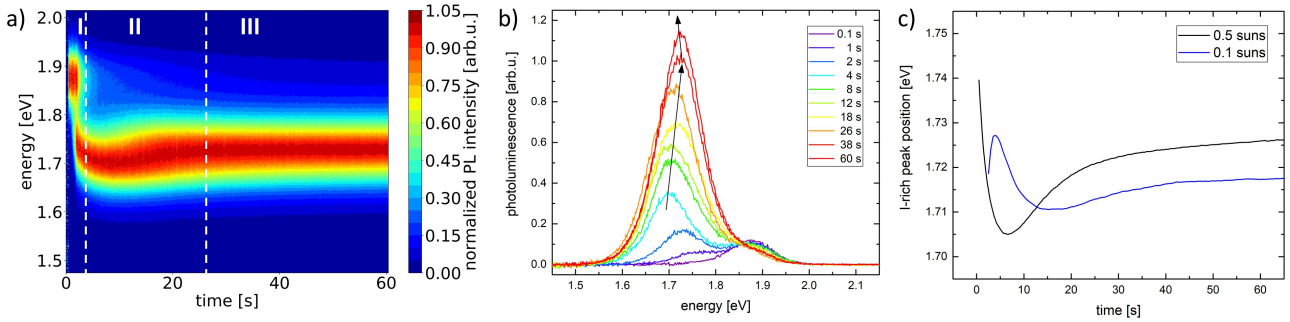

Figure 2. a) Contour plot of individually normalized PL spectra measured on a sample with 'small grains' over 60 seconds under constant illumination of 0.5 suns. b) Several exemplary PL spectra of the same segregation process. c) Peak position of the I-rich luminescence of a sample with 'small grains' measured at 0.1 and 0.5 suns excitation density.

In this study, PL measurements are carried out at 0.1, 0.5, and 5 sun equivalent for both sample types to investigate the influence of the excitation density. Contour plots for each measurement condition are shown normalized in Figure 3 and in linear representation in Figure 4. A general trend, independent of microstructure, is that I-rich luminescence appears faster with increasing excitation density. This trend could indicate increased halide mobility with increasing number of incoming photons.

The PL response during illumination at 0.1 to 0.5 suns is similar over 120 s for the 'small' and 'large grain' samples. Those data sets are fitted with two Gaussians (one for the mixed phase and one for the I-rich luminescence). The respective peak positions are extracted and plotted in Figure 2c) for the 'small grain' sample. For 0.1 suns the blue shift occurs at later times indicating slower kinetics. Further, the magnitude of the blue shift is less pronounced and the final peak position is about 10 meV smaller at 0.5 suns. Looking at the same parameters for the 'large grain' sample, the same trends are found but with a stronger difference of the final peak position (20 meV) between excitation densities. The stronger shift at higher illumination is in line with literature reports finding a faster and more pronounced segregation for higher illumination densities.[29,31,42] It was reported that the illumination density also changes the thermodynamic equilibrium reached after segregation referring to the final composition of the I-rich phase.[36] Interestingly a higher iodide content is found in the final composition for higher excitation densities although the light is the driving force for the segregation.[36] The same trend is observed in our measurements for both sample types which show a ~10 meV higher final I-rich peak position (after 120 s) at 0.5 suns compared to 0.1 suns.

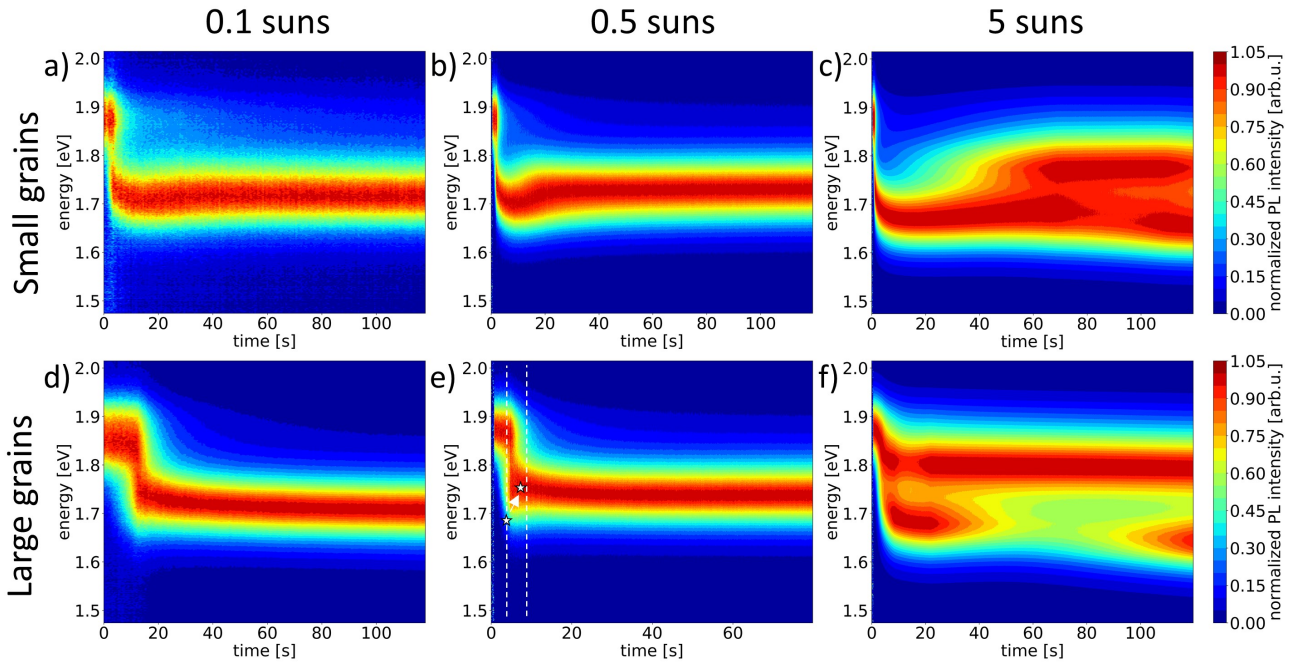

Figure 3. Contour plots of normalized PL spectra of a sample with 'small grain's (a-c) and of a sample with 'large grains' (d-e) measured at 0.1, 0.5, and 5 suns excitation density. The blue shift in stage II is emphasized in e) by 2 stars linked by an arrow.

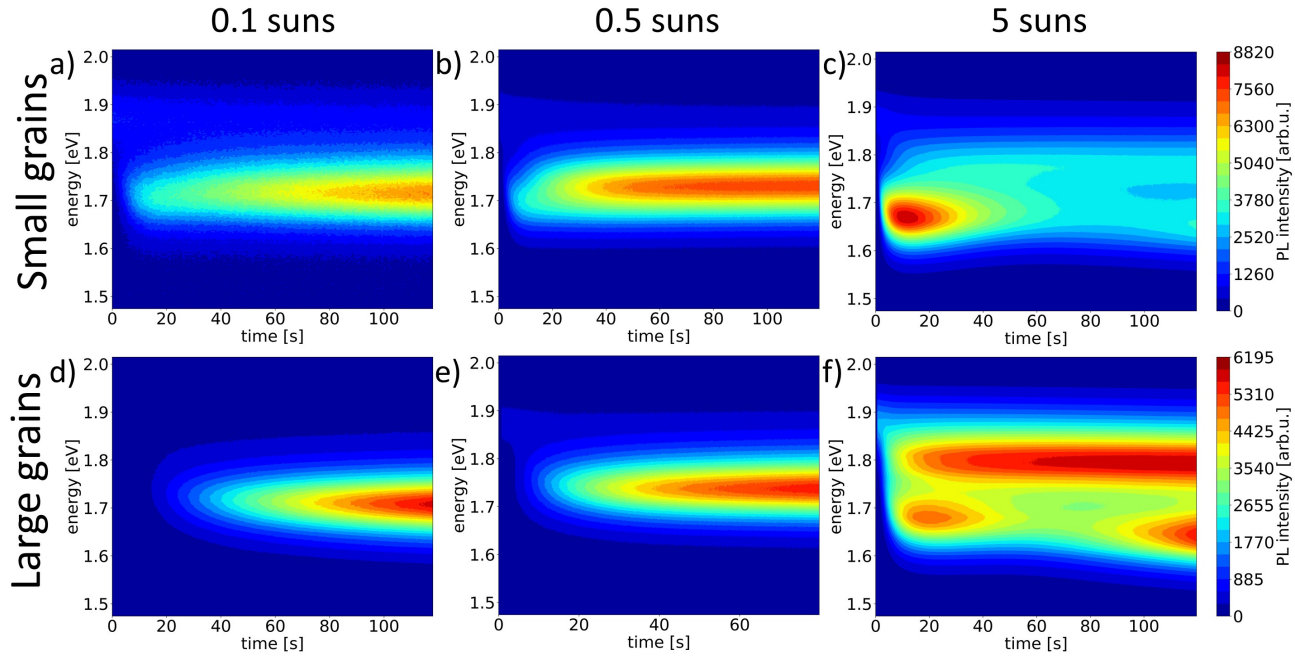

Figure 4. Contour plots of the same data shown in Figure 3 without normalization of the individual spectra. Scaling goes from 0 to the respective maximum value. Shown are PL spectra of a sample with 'small grains' (a-c) and of a sample with 'large grains' (d-e) measured at 0.1, 0.5, and 5 suns excitation density.

Strikingly, the response at 5 suns excitation density is quite different. In case of the 'small grain' sample the initial luminescence from the nearly I-pure domains shifts to much lower energies. Reaching values of ~1.68 eV which corresponds to a Br content of ~20 % (Figures 3c, 4c).[3] This compositions has been widely described as the universal final Br content in a fully segregated sample.[17,28,40,43] It was also proposed in literature that this energy could be related to pure $MAPbI_3$ nanodomains in which quantum confinement effect increase the position of radiative emission.[36] After ~10 sec the luminescence from this peak starts to decrease (Figure 4c) and after 60 seconds a second low energy peak centered ~1.78 eV becomes the main peak (Figure 3c). In the final 20 seconds of the measurement, the peak at 1.68 eV blue shifts towards ~1.64-1.66 eV and increases in intensity.

For the 'large grain' sample a similar change in the segregation dynamics is measured. Upon initial excitation, a strong increase in I-rich luminescence is detected as shown in Figure 4f). However, in this case the two peaks centered at ~1.78 eV and ~1.68 eV are simultaneously present. The higher energy peak in this case is visible, since the emission at ~1.68 eV is weaker compared to the 'small grain' sample (Figure 3f). Also in case of the 'large grain' sample a blue shift is observed for the 1.68 eV emission accompanied by an increase in intensity.

To investigate the convoluted changes in intensity and peak position in more detail the spectra are fitted with Gaussian curves. Unlike for the excitation at 0.1 and 0.5 suns, using two Gaussian profiles (one for the mixed phase and one for the I-rich phase) is not sufficient to properly fit the PL response at 5 suns. Instead a model with three Gaussians is used with some constraints to give reasonable results (Figure 5a). The basis for this model is the superposition of luminescence from clusters with varying halide compositions. This is reasonable because luminescence from clusters with different I-Br ratio has been experimentally shown by Mao et al.[40] In the given model we assume the main contribution to originate from the following three components: nearly I-pure domains, I-rich clusters with higher Br content, and well mixed parts of the pristine sample. The Gaussian describing the well mixed phase is fixed in position (1.87 eV) and FWHM (105 meV) based on the initial peak at 0.1 s and measurements at other excitation densities. To describe the I-rich part of the luminescence (everything below 1.84 eV) two Gaussian are used which FWHM values are between 90 and 120 meV. The position of the two peaks as well as all amplitudes are free fitting parameter. For the following description and the discussion part the two low energy peaks will be referred to as "nearly I-pure domains" for the initial low energy peak and "I-rich clusters" for the Br-enriched clusters that are still I-rich meaning I > 50%.

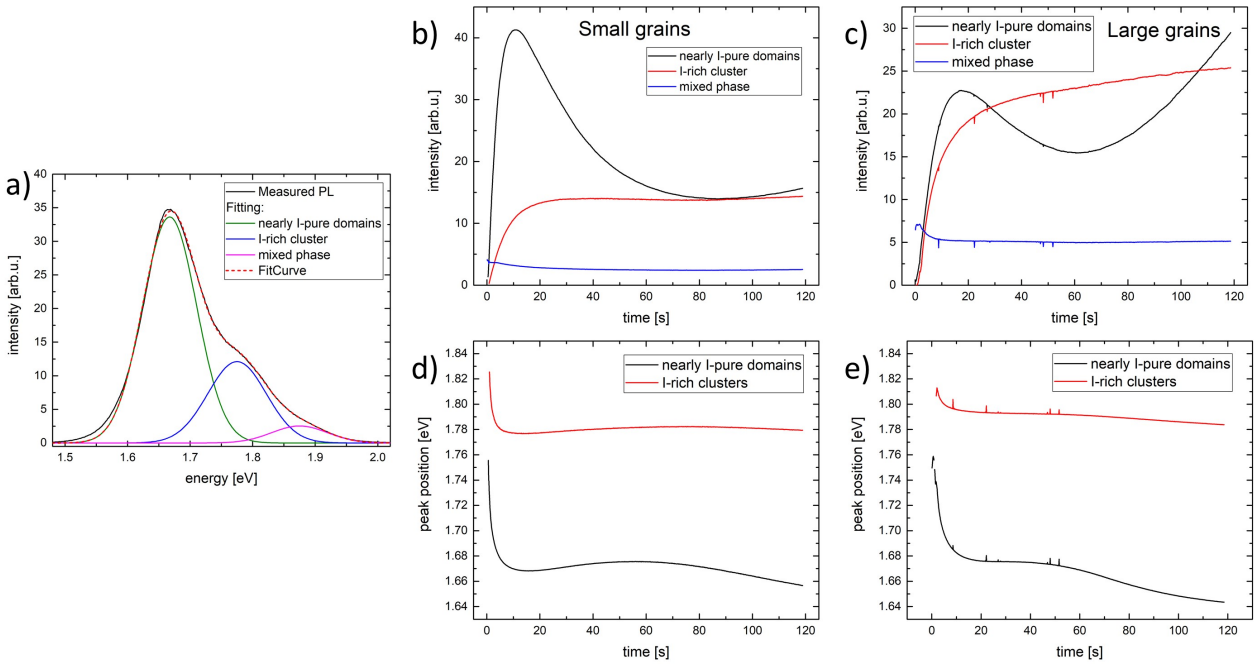

Figure 5. a) PL spectrum measured during halide segregation with high excitation after 30 seconds (black). Added are Gaussian fitting curves representing close to pure I-rich-domains (green), I-rich cluster (blue) and the well mixed phase (pink) as well as the cumulative fit curve as dotted red line. Evolution of the amplitude of the three different Gaussian curves for 'small grains' b) and 'large grains' c). Shift in peak position of the two I-rich peaks for 'small grains' d) and 'large grains' e).

In Figure 5b) the peak maxima of the different Gaussian fits are plotted over time for the 'small grain' sample. The nearly I-pure domains first show a strong increase followed by a gradual decrease. A finding well reflected in the contour plots. Additionally, the behavior of the I-rich clusters can now be quantified showing a steady increase within the first 20 seconds and plateauing afterwards. Plotted in Figure 5d) are the respective peak positions of the two I-rich peaks. The clusters show a red shift within the first seconds which is partly originating from the fitting method. Afterwards the position is stable at 1.78 eV. For the nearly I-pure domains a strong red shift towards 1.67 eV is observed followed by a slight increase by 5 meV. Towards the end the peak red shifts again towards 1.655 eV which is accompanied by an increase in the peak intensity. The luminescence of the mixed phase reduces by roughly 50 % similar to literature reports.[17]

Overall similar observations in terms of intensity and peak position are made for the 'large grain' sample as shown in Figure 5c,e). However, the PL peak of the nearly I-pure domains shows some pronounced differences. The initial rise in intensity is much weaker compared to the 'small grain' sample and is always comparable to the intensity of the I-rich clusters. Another difference is a strong blue shift starting at 60 s reaching values of 1.645 eV. This decrease in peak position. Lastly it should be noted that the intensity of the I-rich clusters continuously increases compared to the 'small grain' sample where it plateaus.

In both cases we link the strongly pronounced increase in intensity to the flash formation of nearly I-pure domains. This process is the same as at lower excitation densities, but the local charge carrier density within the domains is higher now. Since radiative recombination is a bimolecular process it increases super-linearly with a power law factor between 1 and 2.[4,44] Assuming a factor of 2 this means that by increasing charge carrier density by a factor of 10 the radiative recombination increases by a factor of 100. Because of this the nearly I-pure domains have a much higher luminescence yield at high excitation explaining the strong signal. Additionally, a higher number of nearly I-pure domains is likely following the observed trend at 0.1 and 0.5 suns. Since the contribution of the nearly I-pure domains to the PL signal is much higher it is seen as distinct peak (at considerably low energies) instead of broadening the convoluted I-rich peak towards lower energies as seen at 0.1 and 0.5 suns. For the 'small grain' sample, the PL contribution of the nearly I-pure domains is larger. We speculate that this is due to an overall higher number of nearly I-pure domains due to a fast halide segregation along the grain boundaries which facilitates the formation. This assumption follows the earlier findings observing a stronger contribution of the nearly I-pure domains at 0.5 suns.[39]

Over time more clusters with higher Br content form meaning more and more local bandgap minima (~1.78 eV) develop in addition to the global bandgap minima of the nearly I-pure domains (~1.68 eV). This causes the probability of radiative recombination of carriers trapped in local bandgap minima to increase which is reflected by a steady increase in the luminescence centered around 1.78 eV. This process reduces the number of charge carriers within the nearly I-pure domains decreasing the charge carrier density, leading to a significant drop in measured PL signal since the radiative recombination scales with a power law dependence. Other explanations for the decrease in PL would be a dynamical change in composition or also a growth of the nearly I-pure domains which lower the radiative recombination efficiency of the domains due to the incorporation of defects.

For the sample with 'large grains' the peak of the nearly I-pure domains red shifts from 1.675 eV to 1.645 eV between 50 s and 120 s. This final peak position is considerably lower than 1.68 eV (corresponding to 20 % Br) which is commonly observed as the final peak position after segregation.[17,27] Further no segregation is observed in samples with less than 20 % Br content. We propose two possible mechanism for this low bandgap emission. Firstly, this could be correlated to a compositional change in local I-Br ratio based on the fact that the segregation threshold of 20 % Br is not a sharply defined edge. Values as low as 15 % Br or as high as 30 % Br have been reported.[45] The continued shifting towards lower energies can then be explained by a dynamical change in the composition towards lower Br contents. Secondly, this could be related to a loss in quantum confinement. Pure $MAPbI_3$ domains are speculated to form initially but their bandgap is shifted to higher energies due to their small size i.e. quantum confinement effects (< 30 nm).[46] At the later stages of the segregation process those clusters grow in size losing the confinement and thus a red shift occurs. This explanation would follow the description of Suchan et al.[36] The fact that this shift happens only after ~ 60 s, might be explained by a cluster stabilization via trapped carriers.[31] Only when the amount of the trapped carriers reduces, due to the emergence of I-rich clusters, this stabilization is lost leading to domain size growth.

Both, laser-induced local substrate heating and sample degradation can influence the segregation process. We argue to exclude both in our experiment for the following reasons. With a higher temperature the halide mobility strongly increases, facilitating an enhanced formation of nearly I-pure domains (possibly explaining the initially strong luminescence) but also a stronger halide remixing due to compositional gradients (could explain the increase in I-rich

clusters with higher Br as well as the decrease in PL from the nearly I-pure domains). The excitation however is highly localized (0.6 mm) making it likely that the locally generated heat dissipates by diffusion. This explanation is supported by measurement at 50 °C at 0.5 suns which show a similar segregation process compared to room temperature measurement.[39]

Possible is also a sample degradation due to the high excitation density. Measurements by Ruan et al. show that sample degradation is accompanied by the appearance of a PL peak at 2.3 eV corresponding to more stable Br-rich (Br-pure) clusters as well as the disappearance of all other luminescence signals.[47] For the PL spectra measured at 0.1 and 0.5 suns no peak in this energy region is observed. For measurements at 5 suns a tiny peak is detected at 2.15 eV for both sample types which intensity increases for 20 seconds and plateaus afterwards (similarly to the intensity of the I-rich cluster). However, this peak only reaches about ~0.1 % of the I-rich intensity which is comparable to what others have observed for samples that did not degrade.[22] Also humidity which is known to facilitate sample degradation[48,49] should not play a role in our experiments since the perovskite layers were protected by a PMMA coating known to be effective in protecting samples.[31]

4. CONCLUSION

In summary we investigated the influence of excitation density on the halide segregation behavior in $MAPb(I_{0.5}Br_{0.5})_3$ perovskites with different grain sizes. For all cases, a more elaborate segregation process was detected compared to what is typically reported in literature that is a 2 stage process with luminescence of the well mixed phase followed by a continuously red shifting low energy peak. We find an intermediate stage in which luminescence from nearly I-pure domains[36,39] contributes to the overall PL spectra. The multi stage segregation was explained by a dynamically changing superposition of luminescence from clusters with high (35 % - 45 % Br) and low (< 25 % Br) bromide content.

For excitation densities below 0.5 suns, this additional phase of nearly I-pure domains leads to a weak PL signal at low energies which appears before the commonly observed I-rich clusters. The superposition of both signals together with an increase in intensity of the latter leads to blue shift of the I-rich luminescence in this intermediate stage II.[39] The contribution of the nearly I-pure domains reduces over time since more and more I-rich clusters with higher Br content form. The latter act as local carrier traps and recombination centers reducing the charge carrier density and by this the amount of radiative recombination at the nearly I-pure domains. Over time the I-rich clusters start to greatly outnumber the nearly I-pure domains leading to an increase in luminescence from the I-rich cluster to the point where the nearly I-pure domains are not visible anymore. In stage III the Br content inside the clusters reduces and the commonly observed red shift appears.

In case of excitation densities of 5 suns the dynamic interplay between nearly I-pure domains and I-rich clusters is similar but leads to significantly different PL signatures. The PL contribution of the nearly I-pure domains is much higher, due to the bimolecular nature of radiative recombination at the bandgap minima acting as carrier traps. We further speculate that at higher excitation densities more nearly I-pure domains form. Since the PL of the nearly I-pure domains is clearly distinguishable a peak position of ~1.68 eV can be determined. With the same reasoning as for lower excitation densities, the contribution of the nearly I-pure domains diminishes over time as the luminescence from I-rich cluster increases.

Comparing samples with different grain sizes, we find a higher emission intensity of the nearly I-pure domains for samples with higher grain boundary density. We speculate that a higher halide mobility along the grain boundaries aids the formation of the nearly I-pure domains.

We conclude that the light induced halide segregation process is more complex and consits of two separate processes. At the beginning, I-rich clusters from which exhibit a dynamic reduction in Br content over time resulting in a red shift and increase in intensity of the PL peak. In parallel, nearly pure $MAPbI_3$ domains form, leading to a PL peak at much lower energies. The probability to form those nearly iodide pure domains depends on the grain size, temperature and excitation density.

ACKOWLEDGEMENTS

This material is based upon work performed by the Joint Center for Artificial Photosynthesis, a DOE Energy Innovation Hub, supported through the Office of Science of the U.S. Department of Energy under Award Number DE-SC0004993.

REFERENCES

[1] Shirayama, M., Kadowaki, H., Miyadera, T., Sugita, T., Tamakoshi, M., Kato, M., Fujiseki, T., Murata, D., Hara, S., Murakami, T. N., Fujimoto, S., Chikamatsu, M. and Fujiwara, H., "Optical Transitions in Hybrid Perovskite Solar Cells: Ellipsometry, Density Functional Theory, and Quantum Efficiency Analyses for CH3NH3PbI3," Physical Review Applied **5**(1), 014012 (2016).

[2] Yin, W.-J., Shi, T. and Yan, Y., "Unique Properties of Halide Perovskites as Possible Origins of the Superior Solar Cell Performance," Adv. Mater. **26**(27), 4653–4658 (2014).

[3] Noh, J. H., Im, S. H., Heo, J. H., Mandal, T. N. and Seok, S. I., "Chemical Management for Colorful, Efficient, and Stable Inorganic–Organic Hybrid Nanostructured Solar Cells," Nano Letters **13**(4), 1764–1769 (2013).

[4] Sutter-Fella, C. M., Li, Y., Amani, M., Ager, J. W., Toma, F. M., Yablonovitch, E., Sharp, I. D. and Javey, A., "High Photoluminescence Quantum Yield in Band Gap Tunable Bromide Containing Mixed Halide Perovskites," Nano Letters **16**(1), 800–806 (2016).

[5] Fedeli, P., Gazza, F., Calestani, D., Ferro, P., Besagni, T., Zappettini, A., Calestani, G., Marchi, E., Ceroni, P. and Mosca, R., "Influence of the Synthetic Procedures on the Structural and Optical Properties of Mixed-Halide (Br, I) Perovskite Films," J. Phys. Chem. C **119**(37), 21304–21313 (2015).

[6] Stranks, S. D., Eperon, G. E., Grancini, G., Menelaou, C., Alcocer, M. J. P., Leijtens, T., Herz, L. M., Petrozza, A. and Snaith, H. J., "Electron-Hole Diffusion Lengths Exceeding 1 Micrometer in an Organometal Trihalide Perovskite Absorber," Science **342**(6156), 341–344 (2013).

[7] deQuilettes, D. W., Koch, S., Burke, S., Paranji, R. K., Shropshire, A. J., Ziffer, M. E. and Ginger, D. S., "Photoluminescence Lifetimes Exceeding 8 μs and Quantum Yields Exceeding 30% in Hybrid Perovskite Thin Films by Ligand Passivation," ACS Energy Lett. **1**(2), 438–444 (2016).

[8] Brenner, T. M., Egger, D. A., Kronik, L., Hodes, G. and Cahen, D., "Hybrid organic—inorganic perovskites: low-cost semiconductors with intriguing charge-transport properties," Nature Reviews Materials **1**(1), 15007 (2016).

[9] Steirer, K. X., Schulz, P., Teeter, G., Stevanovic, V., Yang, M., Zhu, K. and Berry, J. J., "Defect Tolerance in Methylammonium Lead Triiodide Perovskite," ACS Energy Lett. **1**(2), 360–366 (2016).

[10] Ball, J. M. and Petrozza, A., "Defects in perovskite-halides and their effects in solar cells," Nat Energy **1**(11), 16149 (2016).

[11] National Renewable Energy Laboratory., [Best Research-Cell Efficiencies] (2020).

[12] Hou, Y., Aydin, E., De Bastiani, M., Xiao, C., Isikgor, F. H., Xue, D.-J., Chen, B., Chen, H., Bahrami, B., Chowdhury, A. H., Johnston, A., Baek, S.-W., Huang, Z., Wei, M., Dong, Y., Troughton, J., Jalmood, R., Mirabelli, A. J., Allen, T. G., et al., "Efficient tandem solar cells with solution-processed perovskite on textured crystalline silicon," Science **367**(6482), 1135–1140 (2020).

[13] Quan, L. N., García de Arquer, F. P., Sabatini, R. P. and Sargent, E. H., "Perovskites for Light Emission," Advanced Materials **30**(45), 1801996 (2018).

[14] Zhang, Q., Zhang, D., Fu, Y., Poddar, S., Shu, L., Mo, X. and Fan, Z., "Light Out-Coupling Management in Perovskite LEDs—What Can We Learn from the Past?," Adv. Funct. Mater., 2002570 (2020).

[15] Huang, H., Pradhan, B., Hofkens, J., Roeffaers, M. B. J. and Steele, J. A., "Solar-Driven Metal Halide Perovskite Photocatalysis: Design, Stability, and Performance," ACS Energy Lett. **5**(4), 1107–1123 (2020).

[16] Xing, G., Mathews, N., Lim, S. S., Yantara, N., Liu, X., Sabba, D., Grätzel, M., Mhaisalkar, S. and Sum, T. C., "Low-temperature solution-processed wavelength-tunable perovskites for lasing," Nature Mater **13**(5), 476–480 (2014).

[17] Hoke, E. T., Slotcavage, D. J., Dohner, E. R., Bowring, A. R., Karunadasa, H. I. and McGehee, M. D., "Reversible photo-induced trap formation in mixed-halide hybrid perovskites for photovoltaics," Chemical Science **6**(1), 613–617 (2015).

[18] Unger, E. L., Kegelmann, L., Suchan, K., Sörell, D., Korte, L. and Albrecht, S., "Roadmap and roadblocks for the band gap tunability of metal halide perovskites," Journal of Materials Chemistry A **5**(23), 11401–11409 (2017).

[19] Brennan, M. C., Draguta, S., Kamat, P. V. and Kuno, M., "Light-Induced Anion Phase Segregation in Mixed Halide Perovskites," ACS Energy Letters **3**(1), 204–213 (2018).
[20] Slotcavage, D. J., Karunadasa, H. I. and McGehee, M. D., "Light-Induced Phase Segregation in Halide-Perovskite Absorbers," ACS Energy Lett. **1**(6), 1199–1205 (2016).
[21] DeQuilettes, D. W., Zhang, W., Burlakov, V. M., Graham, D. J., Leijtens, T., Osherov, A., Bulović, V., Snaith, H. J., Ginger, D. S. and Stranks, S. D., "Photo-induced halide redistribution in organic-inorganic perovskite films," Nature Communications **7**(May) (2016).
[22] Yoon, S. J., Draguta, S., Manser, J. S., Sharia, O., Schneider, W. F., Kuno, M. and Kamat, P. V., "Tracking Iodide and Bromide Ion Segregation in Mixed Halide Lead Perovskites during Photoirradiation," ACS Energy Letters **1**(1), 290–296 (2016).
[23] Beal, R. E., Hagström, N. Z., Barrier, J., Gold-Parker, A., Prasanna, R., Bush, K. A., Passarello, D., Schelhas, L. T., Brüning, K., Tassone, C. J., Steinrück, H.-G., McGehee, M. D., Toney, M. F. and Nogueira, A. F., "Structural Origins of Light-Induced Phase Segregation in Organic-Inorganic Halide Perovskite Photovoltaic Materials," Matter **2**(1), 207–219 (2020).
[24] Belisle, R. A., Bush, K. A., Bertoluzzi, L., Gold-Parker, A., Toney, M. F. and McGehee, M. D., "Impact of Surfaces on Photoinduced Halide Segregation in Mixed-Halide Perovskites," ACS Energy Lett. **3**(11), 2694–2700 (2018).
[25] Sutter-Fella, C. M., Ngo, Q. P., Cefarin, N., Gardner, K. L., Tamura, N., Stan, C. V., Drisdell, W. S., Javey, A., Toma, F. M. and Sharp, I. D., "Cation-Dependent Light-Induced Halide Demixing in Hybrid Organic–Inorganic Perovskites," Nano Letters **18**(6), 3473–3480 (2018).
[26] Knight, A. J. and Herz, L. M., "Preventing phase segregation in mixed-halide perovskites: a perspective," Energy Environ. Sci., 10.1039.D0EE00788A (2020).
[27] Brennan, M. C., Ruth, A., Kamat, P. V. and Kuno, M., "Photoinduced Anion Segregation in Mixed Halide Perovskites," Trends in Chemistry **2**(4), 282–301 (2020).
[28] Brennan, M. C., Draguta, S., Kamat, P. V. and Kuno, M., "Light-Induced Anion Phase Segregation in Mixed Halide Perovskites," ACS Energy Lett. **3**(1), 204–213 (2018).
[29] Yang, X., Yan, X., Wang, W., Zhu, X., Li, H., Ma, W. and Sheng, C., "Light induced metastable modification of optical properties in CH3NH3PbI3−xBrx perovskite films: Two-step mechanism," Organic Electronics **34**, 79–83 (2016).
[30] Quitsch, W. A., Dequilettes, D. W., Pfingsten, O., Schmitz, A., Ognjanovic, S., Jariwala, S., Koch, S., Winterer, M., Ginger, D. S. and Bacher, G., "The Role of Excitation Energy in Photobrightening and Photodegradation of Halide Perovskite Thin Films," Journal of Physical Chemistry Letters **9**(8), 2062–2069 (2018).
[31] Knight, A. J., Wright, A. D., Patel, J. B., McMeekin, D. P., Snaith, H. J., Johnston, M. B. and Herz, L. M., "Electronic Traps and Phase Segregation in Lead Mixed-Halide Perovskite," ACS Energy Letters **4**(1), 75–84 (2019).
[32] Elmelund, T., Seger, B., Kuno, M. and Kamat, P. V., "How Interplay between Photo and Thermal Activation Dictates Halide Ion Segregation in Mixed Halide Perovskites," ACS Energy Lett. **5**(1), 56–63 (2020).
[33] Hu, M., Bi, C., Yuan, Y., Bai, Y. and Huang, J., "Stabilized Wide Bandgap MAPbBrxI3–x Perovskite by Enhanced Grain Size and Improved Crystallinity," Adv Sci (Weinh) **3**(6) (2015).
[34] Zhou, Y., Jia, Y.-H., Fang, H.-H., Loi, M. A., Xie, F.-Y., Gong, L., Qin, M.-C., Lu, X.-H., Wong, C.-P. and Zhao, N., "Composition-Tuned Wide Bandgap Perovskites: From Grain Engineering to Stability and Performance Improvement," Advanced Functional Materials **28**(35), 1803130 (2018).
[35] Beal, R. E., Slotcavage, D. J., Leijtens, T., Bowring, A. R., Belisle, R. A., Nguyen, W. H., Burkhard, G. F., Hoke, E. T. and McGehee, M. D., "Cesium Lead Halide Perovskites with Improved Stability for Tandem Solar Cells," J. Phys. Chem. Lett. **7**(5), 746–751 (2016).
[36] Suchan, K., Merdasa, A., Rehermann, C., Unger, E. L. and Scheblykin, I. G., "Complex evolution of photoluminescence during phase segregation of MAPb(I1-xBrx)3 mixed halide perovskite," Journal of Luminescence **221**, 117073 (2020).
[37] Rehman, W., Milot, R. L., Eperon, G. E., Wehrenfennig, C., Boland, J. L., Snaith, H. J., Johnston, M. B. and Herz, L. M., "Charge-Carrier Dynamics and Mobilities in Formamidinium Lead Mixed-Halide Perovskites," Advanced Materials **27**(48), 7938–7944 (2015).
[38] Ruth, A., Brennan, M. C., Draguta, S., Morozov, Y. V., Zhukovskyi, M., Janko, B., Zapol, P. and Kuno, M., "Vacancy-Mediated Anion Photosegregation Kinetics in Mixed Halide Hybrid Perovskites: Coupled Kinetic Monte Carlo and Optical Measurements," ACS Energy Lett. **3**(10), 2321–2328 (2018).

[39] Babbe, F., Masquelier, E., Zheng, Z. and Sutter-Fella, C. M., "Flash formation of I-rich clusters during multi stage halide segregation studied in MAPbI1.5Br1.5," under review at Journal of Physical Chemistry C (2020).
[40] Mao, W., Hall, C. R., Chesman, A. S. R., Forsyth, C., Cheng, Y. B., Duffy, N. W., Smith, T. A. and Bach, U., "Visualizing Phase Segregation in Mixed-Halide Perovskite Single Crystals," Angewandte Chemie - International Edition **58**(9), 2893–2898 (2019).
[41] Mooney, J. and Kambhampati, P., "Get the Basics Right: Jacobian Conversion of Wavelength and Energy Scales for Quantitative Analysis of Emission Spectra," The Journal of Physical Chemistry Letters **5**(20), 3497–3497 (2014).
[42] Slotcavage, D. J., Karunadasa, H. I. and McGehee, M. D., "Light-Induced Phase Segregation in Halide-Perovskite Absorbers," ACS Energy Letters **1**(6), 1199–1205 (2016).
[43] Barker, A. J., Sadhanala, A., Deschler, F., Gandini, M., Senanayak, S. P., Pearce, P. M., Mosconi, E., Pearson, A. J., Wu, Y., Srimath Kandada, A. R., Leijtens, T., De Angelis, F., Dutton, S. E., Petrozza, A. and Friend, R. H., "Defect-Assisted Photoinduced Halide Segregation in Mixed-Halide Perovskite Thin Films," ACS Energy Lett. **2**(6), 1416–1424 (2017).
[44] Draguta, S., Christians, J. A., Morozov, Y. V., Mucunzi, A., Manser, J. S., Kamat, P. V., Luther, J. M. and Kuno, M., "A quantitative and spatially resolved analysis of the performance-bottleneck in high efficiency, planar hybrid perovskite solar cells," Energy Environ. Sci. **11**(4), 960–969 (2018).
[45] Lehmann, F., Franz, A., Többens, D. M., Levcenco, S., Unold, T., Taubert, A. and Schorr, S., "The phase diagram of a mixed halide (Br, I) hybrid perovskite obtained by synchrotron X-ray diffraction," RSC Adv. **9**(20), 11151–11159 (2019).
[46] Parrott, E. S., Patel, J. B., Haghighirad, A.-A., Snaith, H. J., Johnston, M. B. and Herz, L. M., "Growth modes and quantum confinement in ultrathin vapour-deposited $MAPbI_3$ films," Nanoscale **11**(30), 14276–14284 (2019).
[47] Ruan, S., Surmiak, M.-A., Ruan, Y., McMeekin, D. P., Ebendorff-Heidepriem, H., Cheng, Y.-B., Lu, J. and McNeill, C. R., "Light induced degradation in mixed-halide perovskites," J. Mater. Chem. C **7**(30), 9326–9334 (2019).
[48] Yang, J., Siempelkamp, B. D., Liu, D. and Kelly, T. L., "Investigation of CH3NH3PbI3 Degradation Rates and Mechanisms in Controlled Humidity Environments Using in Situ Techniques," ACS Nano **9**(2), 1955–1963 (2015).
[49] Senocrate, A., Acartürk, T., Kim, G. Y., Merkle, R., Starke, U., Grätzel, M. and Maier, J., "Interaction of oxygen with halide perovskites," Journal of Materials Chemistry A **6**(23), 10847–10855 (2018).